ELECTRICAL AND MAGNETIC PROPERTIES

Magneto-Optical Probing of the Magnetic State and Phase Composition of InFeAs Layers

E. A. Gan'shina[a], Z. E. Kun'kova[b, *], I. M. Pripechenkov[a], and Yu. V. Markin[b]

[a] Moscow State University, Moscow, 119991 Russia

[b] Kotel'nikov Institute of Radio Engineering and Electronics, Fryazino Branch, Russian Academy of Sciences, Fryazino, Moscow oblast, 141190 Russia

*e-mail: z.kunkova@gmail.com

Abstract—The spectral, temperature, and magnetic field dependences of the magneto-optical transversal Kerr effect (TKE) have been studied along with the optical spectra of InFeAs layers formed by ion implantation with further pulsed laser melting at different laser pulse energies. A strong dependence of the magneto-optical and optical properties of InFeAs layers on the pulse energy has been revealed. The TKE spectra of the specimen formed at a minimum pulse energy ($W = 0.1$ J/cm^2) indicate the presence of ferromagnetic (In, Fe)As nanoclusters with a Curie temperature of ≈180 K in the weakly doped semiconductive matrix and the absence of secondary magnetic phases. The TKE spectra of layers formed at $W = 0.15–0.4$ J/cm^2 are a superposition of the contributions from ferromagnetic (In,Fe)As nanoareas distributed in the volume and near-surface Fe inclusions. The predominance of the iron contribution in the spectra indicates the intensification of Fe diffusion towards the surface with an increase in the laser pulse energy. Anisotropy in the magneto-optical and optical spectra confirms anisotropic chemical phase separation in the layers.

INTRODUCTION

One of the most important problems in the study of diluted ferromagnetic semiconductors (DFSs) is the synthesis of high-quality materials with intrinsic high-temperature ferromagnetism. Substantial progress has been made in this direction when synthesizing diluted iron-containing DFS $(A^3,Fe)B^5$ (A = Ga, In; B = Sb, As) by low-temperature molecular beam epitaxy [1−6]. In particular, (In,Fe)Sb layers with a Fe content of up to 35% and a Curie point (T_C) above the room temperature (T_{room}) were formed [5]. In the $(A^3,Fe)B^5$ family the (In,Fe)As compound is unique in having both the *p*- and *n*-types of conductivity with a high mobility of electrons [2]. However, (In,Fe)As layers with $T_C > 70$ K cannot be formed by near-uniform doping. At the same time, room-temperature ferromagnetism was found in (In,Fe)As:Be layers grown on vicinal GaAs(001) substrates by spinodal decomposition and delta-doping [6]. If it is possible to create long-range magnetic order in similar layers, they may become promising components of spintronic devices.

(In,Fe)As layers were also grown by ion implantation with further pulsed laser melting (II + PLM). An anisotropic Fe distribution in a semiconductive matrix and a nonzero magnetization at T_{room} were revealed for them [7]. However, it should be taken into account that nanosized inclusions of secondary magnetic phases can be formed under nonequilibrium growth conditions [8, 9]. The appearance of ferromagnetism in DFS layers is usually detected by highly sensitive SQUID-magnetometers and the presence of even a small amount of undesirable magnetic phases can make an appreciable contribution to a magnetic signal and lead to incorrect conclusions. In this connection, the control over the phase composition of diluted ferromagnetic semiconductors is crucially important.

DFS ferromagnetism is exhibited in magneto-optical spectra as singularities, whose location is determined by the energy band structure of an initial semiconductor [10]. For this reason, magneto-optical spectroscopy is an efficient DFS diagnostic and study method, which makes it possible to detect the appearance of ferromagnetism, to study the electron spectrum of a material, and reveal the presence of secondary magnetic phases. We used magneto-optical spectroscopy in the TKE geometry to establish the magnetic state and phase composition of a series of InFeAs specimens. The specimens were manufactured by implanting the same concentration of Fe ions and varying the energy of a laser pulse, which induces the melting and further recrystallization of an implanted layer.

THE SPECIMENS AND METHODS OF THE STUDIES

The specimens were manufactured by the implantation of Fe ions (with an energy of 100 keV and a fluence of $\times 10^{16}$ cm^{-2}) into InAs(001) wafer and the melting using a laser pulse with an energy of $W = 0.1-0.4$ J/cm^2 (step $\Delta W = 0.05$ J/cm^2). Hereinafter, the numbers of specimens correspond to the laser pulse energy (s 0.1–s 0.4). The thickness of recrystallized specimens was ≈ 90 nm. The information about the details of technology and the previous studies of similar specimens is contained in [7], where the presence of the (In,Fe)As phase in the form of lamellae oriented in parallel with InAs plane (110) with a thickness of several nanometers was revealed.

In the experiment we measured the TKE signal

$$\delta = [I(H) - I(-H)]/2I(0), \qquad (1)$$

where $I(H)$ and $I(0)$ are the reflected light intensities in the presence and absence of a magnetic field, respectively, within a range of energies $E = 1.5-3.5$ eV in magnetic fields up to 280 kA/m at the temperatures from 20 to 300 K. The temperature $\delta(T)$ and magnetic field $\delta(H)$ dependences of the transversal Kerr effect were also measured at fixed energies. In view of the anisotropy revealed in [7], the measurements were carried out for two magnetic field orientations with respect to InAs crystallographic axes: **1** for $\vec{H} \parallel [110]$ (light incidence plane $\parallel$ (110)); **2** for $\vec{H} \parallel [1\bar{1}0]$ (incidence plane $\parallel$ (1$\bar{1}$0)). The optical properties of the specimens were studied by spectral ellipsometry. The spectra of the ellipsometry parameters $\Psi(E)$ and $\Delta(E)$ were recorded at room temperature within a range of $E = 1.24-4.5$ eV for the incidence plane orientations **1** $\parallel$ (110) InAs plane and **2** $\parallel$ (1$\bar{1}$0) plane.

RESULTS AND DISCUSSION

Ellipsometry data were used to calculate the spectral dependences of the diagonal components of the pseudodielectric function $\langle\varepsilon\rangle = \langle\varepsilon_1\rangle + i\langle\varepsilon_2\rangle$ of InFeAs specimens. The spectra of the imaginary part $\langle\varepsilon_2(E)\rangle$ for three specimens s 0.1, s 0.2, and s 0.4 demonstrate the common trend of change in the dependences $\langle\varepsilon_2(E)\rangle$ with an increase in the laser pulse energy (Fig. 1). The spectra $\varepsilon_2(E)$ known from the literature for InAs [11] and Fe [12] are also shown in the figure. The energies of transitions E_1, $E_1 + \Delta_1$, and E_0' in the L and X critical points of the InAs Brillouin zone are shown with dashed lines. In the region of these transitions in the spectra $\langle\varepsilon_2(E)\rangle$ there are well pronounced peaks indicating that the energy band structure of InAs is retained in the InFeAs layers formed by the II + PLM method. When the laser pulse energy rises, the $\langle\varepsilon_2(E)\rangle$ values of the layers increase in the low-energy spectral region, where the semiconductive
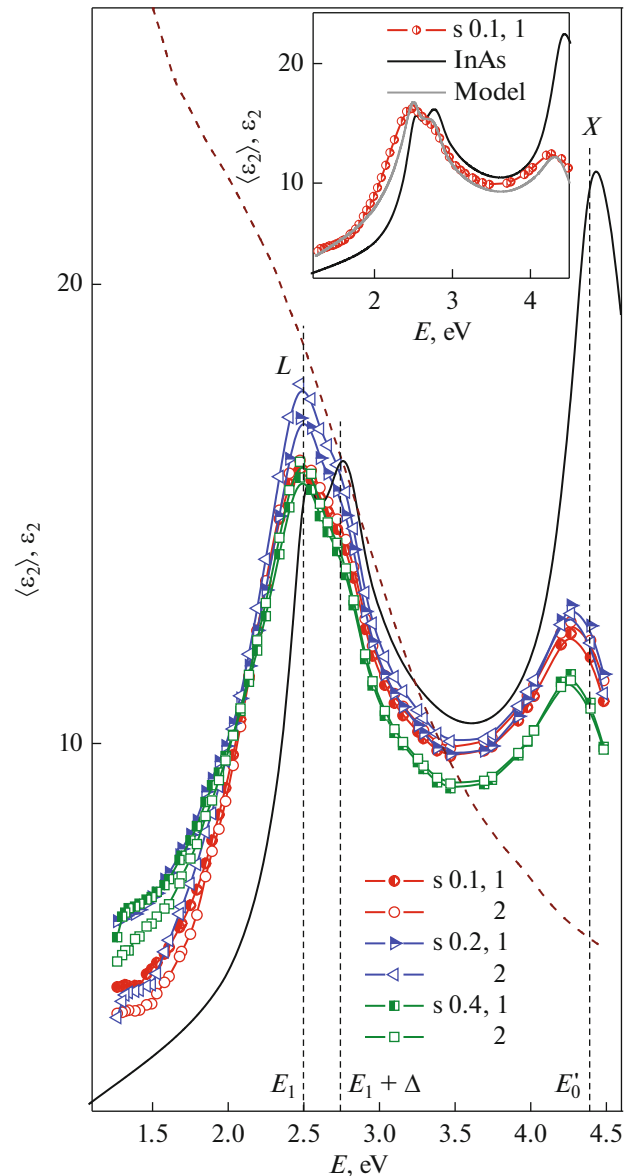

Fig. 1. The spectra of the imaginary part of the pseudodielectric function $\langle\varepsilon_2(E)\rangle$ of specimens s 0.1, s 0.2, and s 0.4 at $T = 300$ K for geometries 1 and 2, InAs spectrum [11] (curve without symbols) and "bulk" iron spectrum [12] (dashed curve) as well as the energies of the transitions E_1, $E_1 + \Delta_1$, and E_0' in InAs at $T = 300$ K (thin dashed lines): (1) incidence plane $\parallel$ InAs plane (110), (2) incidence plane $\parallel$ plane (1$\bar{1}$0). The spectra of specimen s 0.1 and InAs as well as $\langle\varepsilon_2(E)\rangle$ curve for the model composed of an InAs substrate, a 0.8 InAs + 0.2 Fe layer of 2 nm in thickness, and a 0.5 InAs oxides + 0.5 voids mixture layer of 5.5 nm in thickness (inset).

matrix absorption decreases. It can be seen that the doublet produced by the transitions E_1, $E_1 + \Delta_1$ is smeared and the peak in the region of the transition E_0' decreases. A cause of the transformation in the $\langle\varepsilon_2(E)\rangle$ spectra may be an increase in the density of defects in the semiconductive matrix when doping with Fe. It
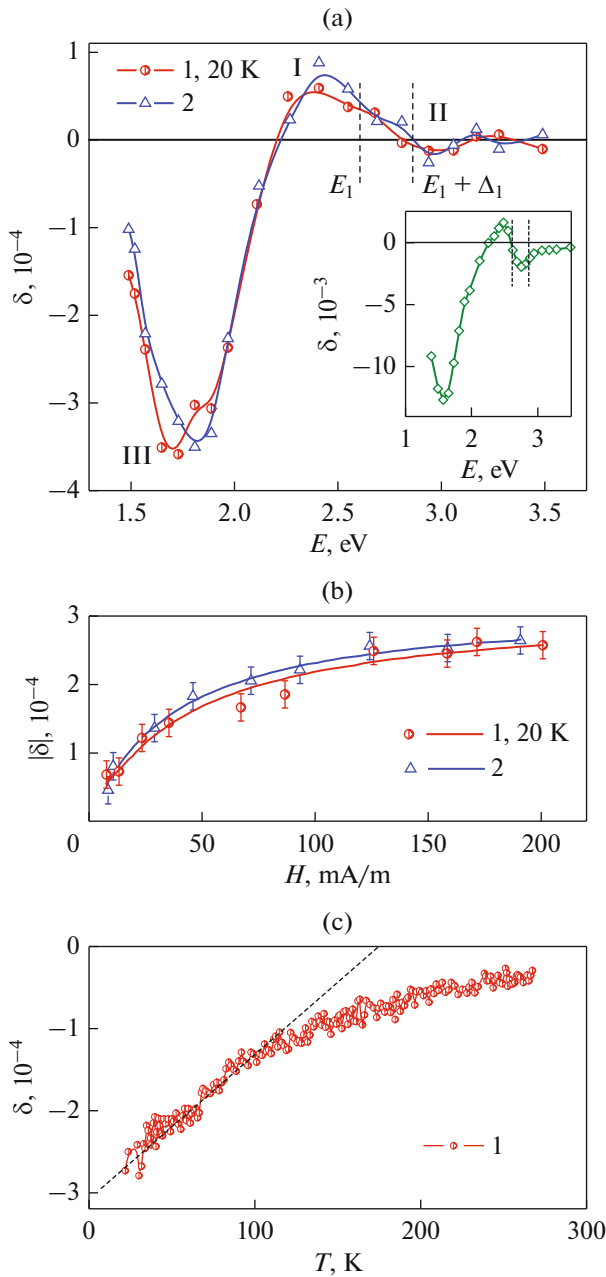
Fig. 2. Specimen s 0.1: (a) TKE spectra at $T = 20$ K and $H = 280$ kA/m for magnetic field orientations (1) $\vec{H} \parallel [110]$, and (2) $\vec{H} \parallel [1\,\overline{1}0]$ with the energies of the E_1 and $E_1 + \Delta_1$ transitions in InAs at $T = 22$ K [13] (dashed lines) as well as the $\delta(E)$ spectrum of the ferromagnetic $In_{0.931}Mn_{0.069}As$ specimen ($T_C = 77$ K) at $T = 17$ K [14] (inset); (b) $\delta(H)$ at $T = 20$ K and $E = 1.81$ eV for orientations 1 and 2 of the field $\vec{H}$ with measurement error (vertical lines); (c) $\delta(T)$ in geometry 1 of the field $H = 200$ kA/m, $E = 1.81$ eV.

follows from the comparison with the Fe spectrum $\varepsilon_2(E)$ that an increase in the $\langle\varepsilon_2\rangle$ values of the layers in the $E < 2.5$ eV region can also be associated with the presence of inclusions retaining the bulk iron proper-

ties in them. The character of the dependences $\langle\varepsilon_2(E)\rangle$ may also be influenced by the presence of oxides and roughness on the layer surface. In addition to the spectrum of specimen s 0.1 in geometry 1 and the spectrum InAs, the inset in Fig. 1 shows the dependence $\langle\varepsilon_2(E)\rangle$ calculated for a model with realistic near-surface area parameters. The model incorporates an InAs substrate, a 0.8 InAs + 0.2 Fe mixture layer 2 nm in thickness, and a near-surface 0.5 InAs oxides + 0.5 voids mixture layer 5.5 nm in thickness. The coefficients specify the volumetric ratio of phases. A rather good agreement between the spectrum $\langle\varepsilon_2(E)\rangle$ of specimen s 0.1 and the model spectrum indicates that the crystal structure in this specimen is slightly damaged. The number of iron inclusions that retain the bulk material properties is small. Uncertainty in the near-surface layer composition for the other specimens did not allow us to construct any models for them. It is only possible to point out that the introduction of a larger amount of Fe into the model leads to a substantial increase of $\langle\varepsilon_2\rangle$ in the low-energy spectral region. It can be seen in Fig. 1 that in the region of $E = 1.24-2.2$ eV, the values of $\langle\varepsilon_2\rangle$ in geometry 1 are higher than in geometry 2, and anisotropy is more pronounced in the spectra of specimen s 0.2.

At room temperature, weak TKE signals were received from all the specimens. The response of specimen s 0.1 at T_{room} was minimal and close to the measurement error. When the temperature decreased, the TKE signals increased. The spectra $\delta(E)$ of specimen s 0.1 at $T = 20$ K and $H = 280$ kA/m in geometries 1 and 2 are shown in Fig. 2a. The spectra contain singularities I and II in the region of the transition energies E_1 (2.608 eV) and $E_1 + \Delta_1$ (2.857 eV) at the L-critical point of the InAs energy band structure, and negative polarity band III in the region of $E \approx 1.5-2.2$ eV. A similar band was observed earlier in the TKE spectra of a ferromagnetic (In,Mn)As semiconductor. For comparison, the $\delta(E)$ spectrum of $In_{0.931}Mn_{0.069}As$ with $T_C = 77$ K [14] is shown in the insert to Fig. 2a. The presence of the characteristic I + II structure in the $\delta(E)$ spectra and the similarity between the spectra of specimen s 0.1 and DFS (In,Mn)As indicate that specimen s 0.1 contains a ferromagnetic phase, i.e., (In,Fe)As. The smallness of the signal from specimen s 0.1 compared to $In_{0.931}Mn_{0.069}As$ with a low for DFS and nearly uniform doping indicates that the content of the (In,Fe)As ferromagnetic phase in specimen s 0.1 is low. The magnetic field dependences $\delta(H)$ at $T = 20$ K and $E = 1.81$ eV for geometries 1 and 2 are shown in Fig. 2b, where the vertical segments show the measurement error equal to $\approx 2 \times 10^{-5}$. The character of the curves $\delta(H)$ can be explained by the magnetic nonuniformity in the specimen, i.e., the presence of paramagnetic and, probably, superparamagnetic phases in addition to the ferromagnetic phase. It can be seen from Figs. 2a and 2b that the spectral and magnetic field dependences of the

transversal Kerr effect of specimen s 0.1 are weakly anisotropic.

The temperature dependences recorded for the transversal Kerr effect of specimen s 0.1 in two geometries coincide with each other within the measurement error. The curve $\delta(T)$ recorded in geometry 1 with the field $H = 280$ kA/m and $E = 1.81$ eV is shown in Fig. 2c. The extrapolation of the region with a more abrupt increase until intersection with the abscissa axis gives an estimate for the Curie temperature of the (In,Fe)As ferromagnetic phase $T_C \approx 180$ K.

The shape of the TKE spectra is substantially transformed with an increase in the laser pulse energy, as comprehensively demonstrated by the dependences $\delta(E)$ of specimen s 0.15 in Fig. 3a. The spectra measured at $T = 50$ and 20 K in geometries 1 and 2 of the field $H = 160$ kA/m represent a broad band of positive polarity with a maximum in the region of 1.7–2.0 eV. In the region of $E < 2.2$ eV, the TKE signals in geometry 1 are appreciably higher than in geometry 2, i.e., magneto-optical anisotropy is well pronounced. The line without symbols in Fig. 3a is the TKE spectrum of a Fe film with a thickness of ≈ 100 nm on a GaAs substrate at T_{room}. The signal from the Fe film was reduced by 22 times. The similarity between the spectra in Fig. 3a indicates that specimen s 0.15 contains iron inclusions retaining the bulk material properties. In the high-energy spectral region, there are weak singularities in the region of the transitions E_1 and $E_1 + \Delta_1$ in InAs. Therefore, the TKE spectra of specimen s 0.15 are a superposition of contributions from Fe inclusions and (In,Fe)As ferromagnetic areas with predominance of the first contribution. In Fig. 3a, it can be seen that the TKE signal is reduced with a decrease in the temperature from 50 to 20 K.

The magnetic field dependences $\delta(H)$ of specimen s 0.15 at $T = 50$ and 20 K in geometries 1 and 2 at $E = 1.97$ eV are shown in Fig. 3b (the measurement error is the same as in Fig. 2b). The character of the dependences $\delta(H)$, which differ from the magnetization curves of iron, can be explained by magnetic and phase nonuniformity in the specimen. The dependence $\delta(T)$ in geometry 1 of the field $H = 160$ kA/m, $E = 1.97$ eV is shown in Fig. 3c. As the temperature is decreased, the transversal Kerr effect sustains an appreciable nearly linear increase replacing with a drop below 50 K. A nonmonotonical temperature behavior of the transversal Kerr effect can be explained by competition between the contributions having positive polarity (from iron inclusions) and negative polarity (from ferromagnetic (In,Fe)As clusters), which become comparable at $T < 50$ K.

The TKE spectra of specimen s 0.2 at $T = 50$ and 300 K in two geometries of the field $H = 200$ kA/m and the reference film spectrum are shown in Fig. 4a. It can be seen that the spectra of specimen s 0.2 are similar to the spectrum of the iron film at both low and room temperatures. The low-temperature spectra of
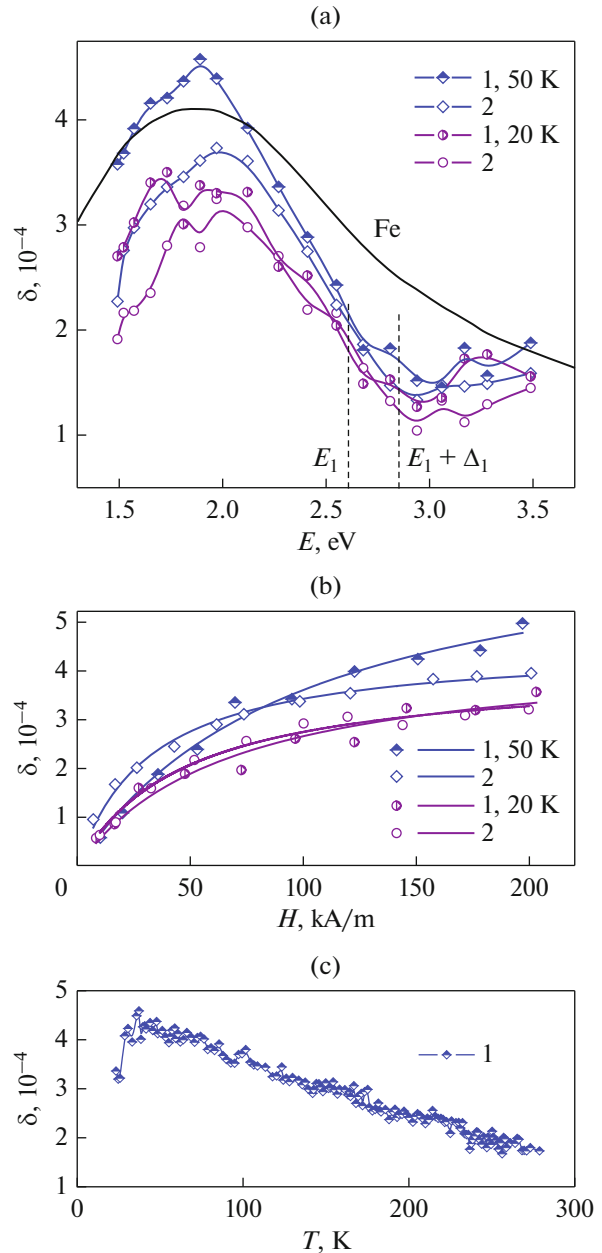

Fig. 3. Specimen s 0.15: (a) TKE spectra at $T = 50$ and 20 K and $H = 160$ kA/m for geometries 1 and 2 and spectrum of a Fe film supported GaAs ($\delta_{Fe}/22$, $d = 100$ nm, $T = 300$ K); (b) $\delta(H)$ for two geometries at $T = 50$ and 20 K and $E = 1.97$ eV; (c) $\delta(T)$ in geometry 1 at $H = 160$ kA/m and $E = 1.97$ eV.

specimen s 0.2 also contain some characteristic singularities in the region of the transitions E_1 and $E_1 + \Delta_1$ in InAs. In the region of $E < 2.2$ eV, the TKE signals in geometry 1 are much higher than in geometry 2. Anisotropy is also well pronounced in the spectra $\langle \varepsilon_2(E) \rangle$ of specimen s 0.2 in Fig. 1. The dependences $\delta(H)$ of specimen s 0.2 at $T = 50$ and 300 K and $E = 1.81$ eV in geometries 1 and 2 are shown in Fig. 4b.
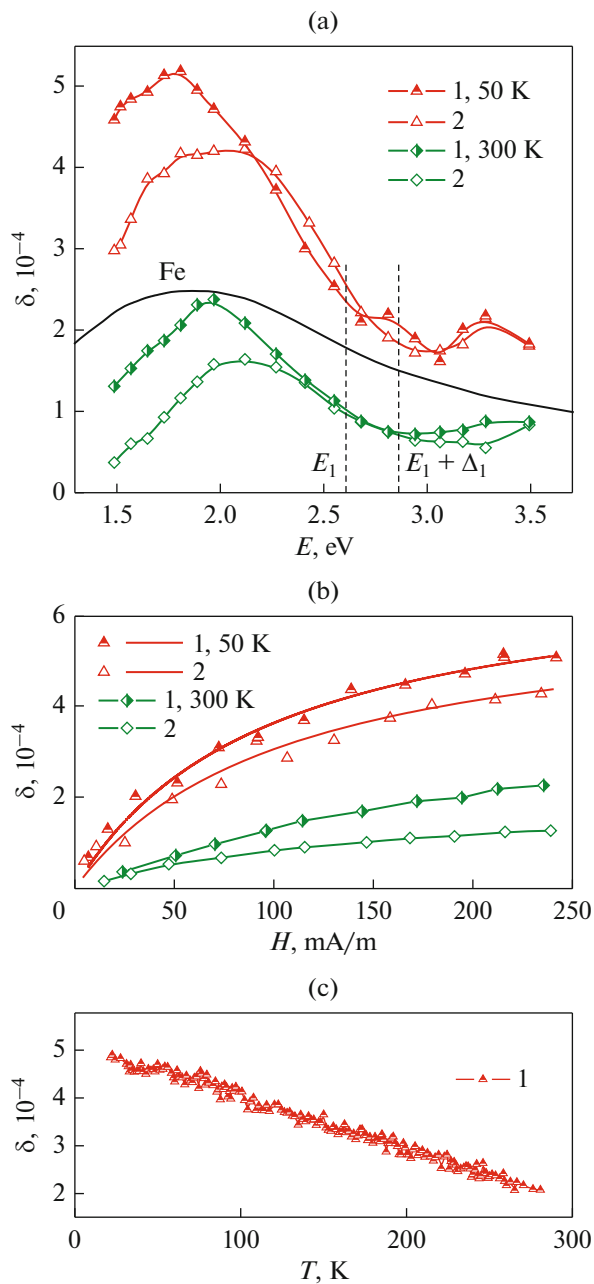
Fig. 4. Specimen s 0.2: (a) TKE spectra in the field $H = 200$ kA/m for geometries 1 and 2 at $T = 50$ and 300 K and spectrum of a Fe film supported GaAs ($\delta_{Fe}/35$, $T = 300$ K) (curve without symbols); (b) $\delta(H)$ for geometries 1 and 2 at $T = 50$ and 300 K and $E = 1.81$ eV; (c) $\delta(T)$ for $H = 200$ kA/m in geometry 1 at $E = 1.97$ eV.

They are similar to the dependences $\delta(H)$ of specimens s 0.1 and s 0.15. The temperature curve $\delta(T)$ of specimen s 0.2 for geometry 1 of the field $H = 200$ kA/m, $E = 1.97$ eV in Fig. 4c demonstrates a substantial linear rise in the TKE signal under cooling. No explicit competition between the contributions of different polarity is exhibited in the TKE spectra and dependences $\delta(H)$ and $\delta(T)$ of specimen s 0.2.

The shape and singularities of the TKE spectra and the character of the dependences $\delta(H)$ and $\delta(T)$, which are observed for specimen s 0.2, are also retained for specimens s 0.25–s 0.4 at both low temperatures and T_{room}. The TKE signal from these specimens is decreased with an increase in the laser pulse energy. Let us point out that the TKE signals from all specimens s 0.15–s 0.4 are small; therefore, the amount of iron inclusions in them is insignificant. We did not reveal them with the use of magnetic force microscopy at T_{room}, probably because of the high locality of this method.

Complex studies of similar InAs films, which were implanted with the same Fe dose and recrystallized in one of the PLM regimes were carried out in [7]. It has been established that ~two-thirds of the Fe atoms diffuse towards the surface after melting, and the residual concentration of the Fe atoms in the InAs layer is ≈ 2.5–3.1%. In the near-surface area of ≈ 50 nm in thickness, approximately 70% of the Fe ions occupy the cation substitution positions. The other the Fe ions are presumably in the defective amorphous surface layer. The InAs matrix was revealed to contain Fe enriched nanocrystals with a thickness of several nanometers and a length of ≈ 90 nm in the form of lamellae parallel to the planes (110). Ferromagnetic coupling inside the iron-enriched nanolamellae was confirmed and the absence of long-range ferromagnetic order in the specimen was established. At T_{room}, nonzero field-induced magnetization was revealed. The theoretical substantiation of the predominant aggregation of the Fe ions along the direction $[1\,\overline{1}0]$ and an anisotropic Fe distribution in the form of iron-enriched lamellae was given. When analyzing our data, we used the results [7].

The characteristic singularities in the region of the transitions at the point L of InAs are present in the low-temperature TKE spectra of all the specimens to confirm that they contain the (In,Fe)As ferromagnetic phase. The (In,Fe)As phase content in the specimens is low, as these singularities are small. Secondary magnetic phases are absent only in specimen s 0.1. The TKE spectrum of this specimen is formed by the (In,Fe)As ferromagnetic inclusions with $T_C \approx 180$ K. The dependences $\delta(H)$ of specimen s 0.1 seem to incorporate the ferromagnetic and superparamagnetic components, whose values are comparable. A slight distinction between the magneto-optical and optical spectra of specimen s 0.1 in two geometries of the experiment agrees with the data in [7], where the coincidence of hysteresis loops was observed in magnetic fields oriented along the axes [110] and $[1\,\overline{1}0]$ corresponding to the equivalence of these directions in the zinc blende structure.

The TKE spectra of specimens s 0.15–s 0.4 are a superposition of contributions from the Fe inclusions and (In,Fe)As. The Fe precipitates can be formed in

the near-surface area, where the concentration of the Fe atoms is increased due to diffusion from the melted layer. According to the energy dispersive X-ray spectroscopy data [7], an increase in the Fe concentration near the surface occurs locally inside the (In,Fe)As nanolamellae. Such a nonuniform Fe distribution in the nanolamellae may lead to an anisotropic distribution of the Fe particles near/on the surface, their alignment with direction [$1\bar{1}0$], and anisotropy in the spectra of specimens s 0.15–s 0.4. No Fe precipitates were revealed in [7]. According to our data, they are present in the specimens manufactured at $W > 0.1$ J/cm^2 (s 0.15–s 0.4).

The increase in the laser pulse energy W from 0.15 to 0.2 J/cm^2 induces the rise in the TKE signal and $\langle\varepsilon_2\rangle$ values, as well as the substantial anisotropy in the magneto-optical and optical spectra. These changes indicate that the amount of the oriented Fe inclusions in the near-surface region rises due to the intensification of diffusion from the melted layer, whose temperature rises with an increase in W. The further increase in W (0.25–0.4 J/cm^2) leads to a decrease in the signals and anisotropy in the TKE spectra with the retention of the spectral shape, the character of the dependences $\delta(H)$ and $\delta(T)$, as well as the increased values of $\langle\varepsilon_2\rangle$ in the low-energy region. Such changes can be produced by the surface diffusion and evaporation of Fe the atoms with an increase in the laser pulse energy. The unusual temperature dependences for the transversal Kerr effect of specimens s 0.2–s 0.4 and the initial region of the curve $\delta(T)$ of specimen s 0.15, which demonstrate substantial linear rise under cooling, are not typical of "bulk" iron (with $T_C = 1043$ K). Perhaps, such a behavior is associated with a rise in the ordering and overall magnetization of noninteracting near-surface ferromagnetic and/or superparamagnetic iron particles in the external magnetic field with decreasing temperature. The magnetic nonuniformity of the layers and comparable values of signals from ferromagnetic and/or superparamagnetic particles and paramagnetic iron atoms seem to determine the character of the TKE–magnetic field dependences of specimens s 0.15–s 0.4.

CONCLUSIONS

A strong effect of the recrystallizing laser pulse energy on the magneto-optical and optical characteristics of the InFeAs II + PLM layers has been revealed. At the minimum pulse energy $W = 0.1$ J/cm^2, the layers with a weakly doped InAs matrix containing ferromagnetic (In,Fe)As nanoclusters with $T_C \approx 180$ K are formed. In these layers, secondary magnetic phases are absent. The specimens manufactured at $W = 0.15$–0.4 J/cm^2 contain the ferromagnetic (In,Fe)As nano-

clusters distributed over the volume and near-surface iron inclusions formed due to the Fe diffusion from the melted layer towards the surface. The anisotropy in the magneto-optical and optical spectra of the specimens manufactured at $W = 0.15$–0.4 J/cm^2 corresponds to the picture of anisotropic chemical phase separation [7]. This indicates that the Fe diffusion occurs from the regions where the iron-enriched crystallographically oriented (In,Fe)As nanolamellae are formed, which leads to the formation of the oriented iron nanoclusters near and/or on the surface. The nonmonotonical dependence of the TKE signal on the laser pulse energy for the specimens prepared at $W > 0.1$ J/cm^2 may result from the surface diffusion and evaporation of the Fe atoms with an increase in the pulse energy.

REFERENCES

1. P. N. Hai, L. D. Anh, S. Mohan, T. Tamegai, M. Kodzuka, T. Ohkubo, K. Hono, and M. Tanaka, "Growth and characterization of n-type electron-induced ferromagnetic semiconductor (In,Fe)As," Appl. Phys. Lett. **101**, 182403 (2012).

2. P. N. Hai, L. D. Anh, and M. Tanaka, "Electron effective mass in n-type electron-induced ferromagnetic semiconductor (In,Fe)As: Evidence of conduction band transport," Appl. Phys. Lett. **101**, 252410 (2012).

3. S. Sakamoto, L. D. Anh, P. N. Hai, G. Shibata, Y. Takeda, M. Kobayashi, Y. Takahashi, T. Koide, M. Tanaka, and A. Fujimori, "Magnetization process of the n-type ferromagnetic semiconductor (In,Fe)As:Be studied by X-ray magnetic circular dichroism," Phys. Rev. B **93**, 035203 (2016).

4. N. T. Tu, P. N. Hai, L. D. Anh, and M. Tanaka, "High-temperature ferromagnetism in heavily Fe-doped ferromagnetic semiconductor (Ga,Fe)Sb," Appl. Phys. Lett. **108**, 192401 (2016).

5. N. T. Tu, P. N. Hai, L. D. Anh, and M. Tanaka, "Heavily Fe-doped ferromagnetic semiconductor (In,Fe)Sb with high Curie temperature and large magnetic anisotropy," Appl. Phys. Exp. **12**, 103004 (2019).

6. P. N. Hai, M. Yoshida, A. Nagamine, and M. Tanaka, "Inhomogeneity-induced high temperature ferromagnetism in n-type ferromagnetic semiconductor (In,Fe)As grown on vicinal GaAs substrates," Jpn. J. Appl. Phys. **59**, 063002 (2020).

7. Y. Yuan, R. Hübner, M. Birowska, Ch. Xu, M. Wang, S. Prucnal, R. Jakiela, K. Potzger, R. Böttger, S. Facsko, J. A. Majewski, M. Helm, M. Sawicki, Sh. Zhou, and T. Dietl, "Nematicity of correlated systems driven by anisotropic chemical phase separation," Phys. Rev. Mater. **2**, 114601 (2018).

8. T. Dietl, K. Sato, T. Fukushima, A. Bonanni, M. Jamet, A. Barski, S. Kuroda, M. Tanaka, P. N. Hai, and H. Katayama-Yoshida, "Spinodal nanodecomposition in semiconductors doped with transition metals," Rev. Mod. Phys. **87**, 1311−1377 (2015).

9. L. M. C. Pereira, "Experimentally evaluating the origin of dilute magnetism in nanomaterials," J. Phys. D: Appl. Phys. **50**, 393002 (2017).

10. K. Ando, *Magneto-Optics of Diluted Magnetic Semiconductors: New Materials and Applications, Magneto-Optics*, Ed. by S. Sugano and N. Kojima (Springer, Berlin, 2000), Vol. 128, pp. 211−241.

11. E. D. Palik and R. T. Holm, *Indium arsenide, Handbook of Optical Constants of Solids*, Ed. by E. D. Palik (Academic, Orlando, 1985), pp. 479−489.

12. P. B. Johnson and R. W. Christy, "Optical constants of transition metals: Ti, V, Cr, Mn, Fe, Co, Ni, and Pd," Phys. Rev. B **9**, 5056−5070 (1974).

13. T. J. Kim, J. J. Yoon, S. Y. Hwang, Y. W. Jung, T. H. Ghong, Y. D. Kim, H. J. Kim, and Y.-C. Chang, "InAs critical-point energies at 22 K from spectroscopic ellipsometry," Appl. Phys. Lett. **97**, 171912 (2010).

14. E. A. Gan'shina, L. L. Golik, Z. E. Kun'kova, G. S. Zykov, A. I. Rukovishnikov, and Yu. V. Markin, "Magnetic inhomogeneity manifestations in the magneto-optical spectra of (In−Mn)As layers," IEEE Magn. Lett. **11**, 2502105 (2020).

Translated by E. Glushachenkova